Effective diffusivity in non-isotropic gradient flows

1995 J. Phys. A: Math. Gen. 28 6013

(http://iopscience.iop.org/0305-4470/28/21/009)

J. Phys. A: Math. Gen. 28 (1995) 6013–6025. Printed in the UK

Effective diffusivity in non-isotropic gradient flows

D S Dean†‡, I T Drummond† and R R Horgan†

† Department of Applied Mathematics and Theoretical Physics, University of Cambridge, Silver Street, Cambridge CB3 9EW, UK

‡ Service de Physique de l'Etat Condensé, CEA-Saclay, 91191 Gif-sur-Yvette Cedex, France

Received 12 April 1995

Abstract. We study the effective diffusivity tensor for particles in a random gradient flow that, statistically, lacks rotational symmetry. The effective diffusivity tensor is computed up to two-loop order in perturbation theory and the 'Ward identity' that relates this tensor to the effective coupling is verified to the same order.

We re-examine the renormalization group calculation that produced a very accurate numerical value for the effective diffusivity in the rotationally symmetric case and formulate two versions based on distinct divisions of the random potential field that gives rise to the flow. Both types of renormalization group calculation give good results when compared with numerical simulations. However, at two-loop order in perturbation theory the two methods differ in detail from each other and from the exact perturbation calculation. This is in contrast to the corresponding results in the isotropic case.

1. Introduction

Recently, work on the problem of advective diffusion of scalar fields in random velocity fields [4–6, 9] has arrived at some interesting and apparently exact results in the case of gradient flow that is statistically rotationally invariant (as well as translation invariant). This work complements that on anomalous diffusion reviewed in [1].

In this paper we extend some of these results to the case of gradient flow for which the assumption of statistical isotropy does not hold. This study is not only interesting in its own right but also provides a wider context in which to view the previously successful calculations. We analyse the difficulties and discrepancies that enter in the new, physically more complex, situation.

2. *Green functions*

The equation for the (conjugate) Green function in a velocity field $\boldsymbol{u}(\boldsymbol{x}) = \lambda_0 \nabla\phi(\boldsymbol{x})$ is

$$\big(\kappa_0 \nabla^2 - \lambda_0 \nabla\phi(\boldsymbol{x}) \cdot \nabla\big) G(\boldsymbol{x}, \boldsymbol{x}') = -\delta(\boldsymbol{x} - \boldsymbol{x}') \,. \tag{1}$$

After averaging over the random ensemble of flows we obtain an effective Green function

$$\mathcal{G}(\boldsymbol{x} - \boldsymbol{x}') = \langle G(\boldsymbol{x}, \boldsymbol{x}') \rangle \sim \frac{1}{4\pi\sqrt{\det\kappa\,(\kappa^{-1})_{ij}(\boldsymbol{x} - \boldsymbol{x}')_i(\boldsymbol{x} - \boldsymbol{x}')_j}} \qquad \text{for} \quad |\boldsymbol{x} - \boldsymbol{x}'| \to \infty \tag{2}$$

where κ_{ij} is the effective diffusivity tensor that controls the long-range dispersal of the scalar field. The Fourier transform of $\mathcal{G}(\boldsymbol{x}-\boldsymbol{x}')$ is

$$\tilde{\mathcal{G}}(\boldsymbol{k}) = [\kappa_0 k^2 - \Sigma(\boldsymbol{k})]^{-1} . \tag{3}$$

At small $\boldsymbol{k}$ the irreducible two-point function $\Sigma(\boldsymbol{k})$ satisfies

$$\Sigma(\boldsymbol{k}) \sim \sigma_{ij} k_i k_j \tag{4}$$

with the result that the effective long-range diffusivity is

$$\kappa_{ij} = \kappa_0 \delta_{ij} - \sigma_{ij} . \tag{5}$$

For the purposes of simulation we assumed that the scalar field correlator $\Delta(\boldsymbol{x}-\boldsymbol{x}') \equiv \langle\phi(\boldsymbol{x})\phi(\boldsymbol{x}')\rangle$ has the form

$$\Delta(\boldsymbol{x}-\boldsymbol{x}') = \int \frac{\mathrm{d}^3 q}{(2\pi)^3} D(q)\, \mathrm{e}^{\mathrm{i}\boldsymbol{q}\cdot(\boldsymbol{x}-\boldsymbol{x}')} \tag{6}$$

with

$$D(q) = (2\pi)^{3/2} (\det A)^{1/2}\, \mathrm{e}^{-q_i A_{ij} q_j/2} . \tag{7}$$

The normalization is chosen so that

$$\langle(\phi(\boldsymbol{x}))^2\rangle = 1 . \tag{8}$$

In our simulations we chose the symmetric matrix A to be diagonal in the coordinate basis.

3. Graphical rules for perturbation theory

The Feynman rules for the diagrammatic perturbation expansion are essentially the same as in the isotropic case. We have

(i) The sum of the inwardly flowing wavevectors at each vertex is zero.

(ii) Each full line carries a factor of $1/\kappa_0 k^2$.

(iii) Each loop wavevector q is integrated with a factor $\mathrm{d}^3 q/(2\pi)^3$.

(iv) Each vertex of the form of figure 1 carries a factor $\lambda_0\, (\boldsymbol{k}+\boldsymbol{q}) \cdot \boldsymbol{q}$.

(v) Each broken line carries a factor $D(q)$.

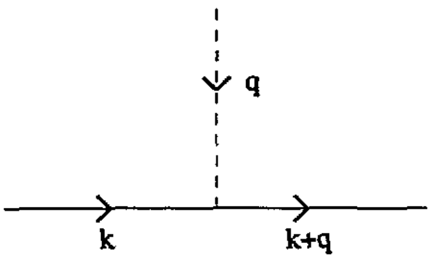

Figure 1. Vertex diagram.

4. One-loop contributions

The calculation for the one-loop contribution to $\Sigma(\boldsymbol{k})$ is also much the same as the isotropic case except that we only make use of the symmetry $D(-q) = D(q)$ in manipulating the integrand. The one-loop contribution to $\Sigma(\boldsymbol{k})$ is associated with the diagram in figure 2. From the above rules we have

$$\Sigma^{(1)}(\boldsymbol{k}) = -\frac{\lambda_0^2}{\kappa_0} \int \frac{\mathrm{d}^3 q}{(2\pi)^3} D(q) \frac{(\boldsymbol{k}+\boldsymbol{q})\cdot\boldsymbol{q}\ \boldsymbol{k}\cdot\boldsymbol{q}}{(\boldsymbol{k}+\boldsymbol{q})^2} . \tag{9}$$

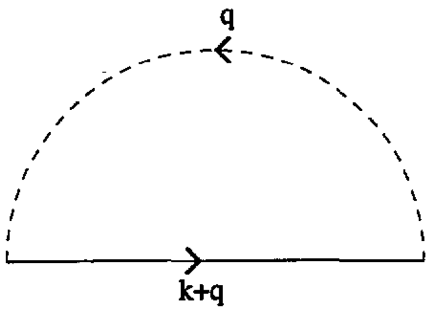

Figure 2. One-loop contribution to Σ.

Using the same manipulations as in [5] we find to $O(k^2)$ the result

$$\Sigma^{(1)}(\boldsymbol{k}) \simeq \frac{\lambda_0^2}{\kappa_0} \int \frac{\mathrm{d}^3 q}{(2\pi)^3} D(q) \frac{\boldsymbol{k}\cdot\boldsymbol{q}\ \boldsymbol{k}\cdot\boldsymbol{q}}{q^2} . \tag{10}$$

This can be expressed as

$$\Sigma^{(1)}(\boldsymbol{k}) \simeq \frac{\lambda_0^2}{\kappa_0} \rho_{ij} k_i k_j \tag{11}$$

where

$$\rho_{ij} = \int \frac{\mathrm{d}^3 q}{(2\pi)^3} D(q) \frac{q_i\ q_j}{q^2} . \tag{12}$$

The one-loop calculation for the diffusivity tensor is then

$$\kappa_{ij} = \kappa_0 \left\{ \delta_{ij} - \frac{\lambda_0^2}{\kappa_0^2} \rho_{ij} \right\} . \tag{13}$$

It is of interest to note that the trace κ_{ii} is identical with the result for the isotropic case, namely

$$\kappa_{ii} = 3\kappa_0 \left\{ 1 - \frac{\lambda_0^2}{3\kappa_0^2} \Delta(0) \right\} \tag{14}$$

where we have used the obvious result

$$\rho_{ii} = \int \frac{\mathrm{d}^3 q}{(2\pi)^3} D(q) = \Delta(0) . \tag{15}$$

5. Two-loop contributions

The two-loop contributions to $\Sigma(\boldsymbol{k})$ are associated with figures 3(a) and (b). With minor changes they can also be manipulated in much the same way as for the isotropic case. We omit the details of these calculations. From the two-loop $O(k^2)$ contribution to $\Sigma(\boldsymbol{k})$ we obtain to this order the result for the effective diffusivity tensor

$$\kappa_{ij} = \kappa_0 \left\{ \delta_{ij} - \frac{\lambda_0^2}{\kappa_0^2} \rho_{ij} + \frac{1}{2} \frac{\lambda_0^4}{\kappa_0^4} \rho_{im} \rho_{mj} + \frac{\lambda_0^4}{\kappa_0^4} \nu_{ij} \right\} \tag{16}$$

where

$$\nu_{ij} = \frac{1}{2} \left\{ \int \frac{\mathrm{d}^3 q}{(2\pi)^3} \frac{\mathrm{d}^3 p}{(2\pi)^3} D(\boldsymbol{q}) D(\boldsymbol{p}) \frac{[p_i q_m - q_i p_m] q_m\ \boldsymbol{q}\cdot\boldsymbol{p}\ q_j}{q^2\ (\boldsymbol{q}+\boldsymbol{p})^2\ q^2} + (i \leftrightarrow j) \right\} . \tag{17}$$

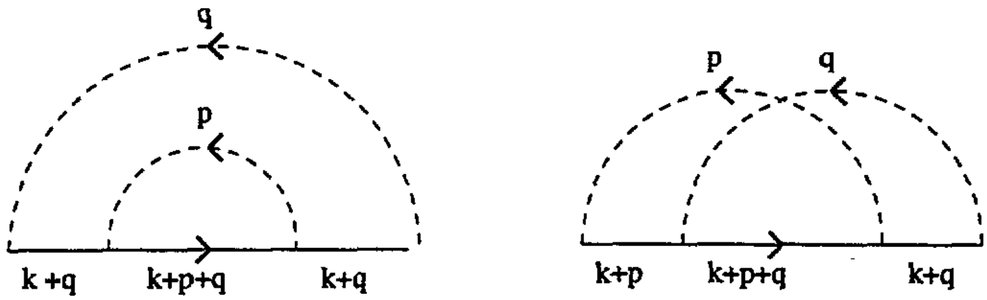

(*a*) (*b*)

Figure 3. Two-loop contributions to Σ.

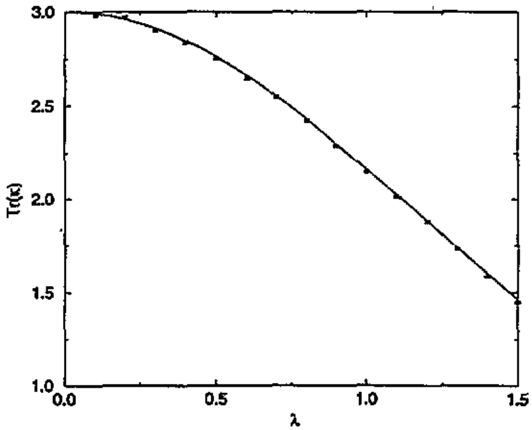

Figure 4. $\mathrm{Tr}(\kappa)$ versus $\mathrm{Tr}\exp\left(-\lambda_0^2\rho\right)$.

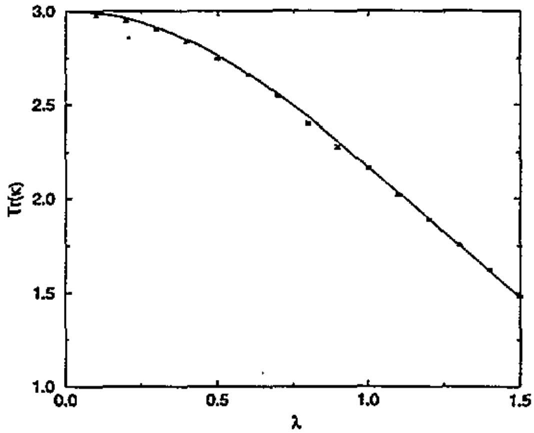

Figure 5. $\mathrm{Tr}(\kappa)$ versus $\mathrm{Tr}\exp\left(-\lambda_0^2\rho\right)$.

An important feature of the above calculation is that the trace $\nu_{ii} = 0$. Note that, as expected, ν_{ij} vanishes in the isotropic case. It therefore follows that

$$\kappa_{ii} = \kappa_0 \,\mathrm{Tr}\left\{1 - \frac{\lambda_0^2}{\kappa_0^2}\rho + \frac{1}{2}\frac{\lambda_0^4}{\kappa_0^4}\rho^2 + \cdots\right\}. \qquad (18)$$

This suggests the result

$$\kappa_{ii} = \kappa_0 \operatorname{Tr} \exp\left\{-\frac{\lambda_0^2}{\kappa_0^2}\rho\right\}. \tag{19}$$

It is of course consistent with the result for the isotropic case. A comparison of this prediction with the results of the simulation for various parameters is shown in figures 4 and 5.

6. 'Ward' identity

As explained in [5] the complete vertex function of the theory has the form

$$V(q, k') = q_i V_i(q, k') \tag{20}$$

where

$$V_i(q, k') = W_{ij}(q, k') k'_j . \tag{21}$$

However, we no longer have rotational invariance for the system. It follows that we cannot expect $W_{ij}(0, 0) \propto \delta_{ij}$. In general, we must allow for the presence of a tensor coupling λ_{ij} at low momentum, thus

$$V_i(0, k) = \lambda_{ij} k_j \tag{22}$$

as $k \to 0$. This corresponds to an effective coupling, induced by the averaging procedure over the fluctuating field, of the form

$$-\lambda_{ij} \partial_i \phi_B(x) \partial_j$$

that appears in the equation for the effective Green function in the presence of a background field $\phi_B(x)$.

In the isotropic case we were able to prove to two-loop order the 'Ward' identity

$$\frac{\partial}{\partial k_i}\Sigma(k) = -2(\kappa_0/\lambda_0)[V_i(0, k) - \lambda_0 k_i] + U_i(k) \tag{23}$$

where

$$U_i(k) \sim O(k^2) k_i \tag{24}$$

as $k \to 0$. The method of proof apparently relied on the isotropy of $D(q)$. However, a careful examination of the terms in the expansion shows that reflection symmetry is sufficient and the result remains true in the present non-isotropic case. The calculations are along the same lines as those in [5] and we omit the details.

The Ward identity (equation (23)) can be more conveniently written as

$$\frac{\partial}{\partial k_i}[\mathcal{G}(k)]^{-1} = 2(\kappa_0/\lambda_0) V_i(0, k) - U_i(k) . \tag{25}$$

Taking account of the low-momentum behaviour of $\mathcal{G}(k) \simeq k_i k_j \kappa_{ij}$ we see that the Ward identity implies that

$$\kappa_{ij} = (\kappa_0/\lambda_0)\lambda_{ij} . \tag{26}$$

In other words the Ward identity implies that the effective coupling tensor λ_{ij} is proportional to the effective diffusivity tensor. This is a somewhat remarkable result in view of the intrinsically non-isotropic contribution, ν_{ij}, to the effective diffusivity tensor.

It is important for the truth of the Ward identity and the proportionality property that the breakdown of isotropy is due entirely to the statistics of the fluctuating field $\phi(x)$. If there were further removal of isotropy due to the presence of a tensorial diffusion constant at the molecular level then any resulting Ward identity would have a more complicated structure and the implications for the effective tensors would be correspondingly less straightforward.

7. Renormalization group calculation

Armed with the equality $\kappa_{ij} = (\kappa_0/\lambda_0)\lambda_{ij}$ that must hold between the running values of the diffusivity tensor and the coupling tensor it is a simple matter to formulate a generalization of the renormalization group argument that proved successful in calculating the effective diffusivity in the isotropic case.

The basis of the renormalization group method is the division of the Gaussian process giving rise to the field $\phi(x)$ into infinitesimal elements based on the magnitude of the associated wavenumber Λ. The running value of the effective diffusivity is that associated with the effect of all the fluctuations of $\phi(x)$ with wavenumbers above Λ. We will investigate this 'momentum' slicing method here.

We point out, however, that other methods of division are also possible. For example, it is perfectly valid to divide $\phi(x)$ into a set of independent Gaussian processes based on some arbitrary parameter, t say, with the range $0 \leqslant t \leqslant 1$. We can write

$$\phi(x) = \int_0^1 \mathrm{d}t\, \phi_t(x) \tag{27}$$

where

$$\langle \phi_t(x)\phi_{t'}(x')\rangle = \delta(t-t')\Delta(x-x') . \tag{28}$$

We then introduce running parameters that depend on t, $\kappa_{ij}(t)$ and $\lambda_{ij}(t)$, and require that $\kappa_{ij}(0) = \kappa_0\delta_{ij}$ and $\lambda_{ij}(0) = \lambda_0\delta_{ij}$. In the isotropic case we can use either division to obtain the same result. In the non-isotropic case that we discuss here, the latter division of $\phi(x)$ has the advantage of being a little simpler than the momentum slicing metnod.

The basis for the renormalization group calculation is the change in $\Sigma(k)$ that results from a change in the correlation function $D(q)$. This is calculated from the diagram in figure 1 with an appropriate reinterpretation of the lines and vertices. The broken line now corresponds to $\delta D(q)$, the vertices now involve the running coupling tensor $\lambda_{ij} = (\lambda_0/\kappa_0)\kappa_{ij}$ where we have suppressed the dependence on the running parameter. The full line corresponds to the the effective propagator which has the form

$$\frac{1}{(q+k)_m\kappa_{mn}(q+k)_n} .$$

The result is that the change in $\Sigma(k)$ is

$$\delta\Sigma(k) = -\frac{\lambda_0^2}{\kappa_0^2}\int \frac{\mathrm{d}^3q}{(2\pi)^3}\delta D(q)\frac{q_l\kappa_{lm}(q+k)_m\; q_n\kappa_{nj}k_j}{(q+k)_m\kappa_{mn}(q+k)_n} . \tag{29}$$

In the above integrand the diffusivity tensor κ_{ij} replaces δ_{ij} in the standard one-loop integral. This makes it possible to repeat the standard manipulation employed above and write

$$q_l\kappa_{lm}(q+k)_m = (q+k)_l\kappa_{lm}(q+k)_m - k_l\kappa_{lm}(q+k)_m . \tag{30}$$

We then have

$$\delta\Sigma(k) = -\frac{\lambda_0^2}{\kappa_0^2}\int \frac{\mathrm{d}^3q}{(2\pi)^3}\delta D(q)\left\{q_n\kappa_{nj}k_j - \frac{k_l\kappa_{lm}(q+k)_m\; q_n\kappa_{nj}k_j}{(q+k)_m\kappa_{mn}(q+k)_n}\right\} . \tag{31}$$

The first term vanishes because of the symmetry of $\delta D(q)$ under reflections in q with the result

$$\delta\Sigma(k) = \frac{\lambda_0^2}{\kappa_0^2}\int \frac{d^3q}{(2\pi)^3}\delta D(q)\frac{k_i\kappa_{im}q_m\ q_n\kappa_{nj}k_j}{q_m\ \kappa_{mn}\ q_n}\,. \tag{32}$$

In the momentum (or wavenumber) slicing version of the renormalization group calculation

$$\delta D(q) = \delta\Lambda\delta(\Lambda - q)D(q)\,. \tag{33}$$

The current value of the diffusivity tensor is influenced by effects at wavenumbers greater than Λ so the effect of the new slice $\delta D(q)$ is to make the shift $\Lambda \to \Lambda - \delta\Lambda$. In these circumstances

$$\delta\Sigma(k) = +\delta\Lambda\frac{d\kappa_{ij}}{d\Lambda}k_ik_j \tag{34}$$

for small k. As a result we have

$$\frac{d\kappa_{ij}}{d\Lambda} = \frac{\lambda_0^2}{\kappa_0^2}\int \frac{d^3q}{(2\pi)^3}\delta(\Lambda - q)D(q)\frac{\kappa_{im}q_m\ q_n\kappa_{nj}}{q_m\ \kappa_{mn}\ q_n}\,. \tag{35}$$

The renormalization group prediction for the effective diffusivity is $\kappa_{ij}(\Lambda = 0)$, obtained by integrating this differential equation and imposing the boundary condition $\kappa_{ij}(\Lambda = \infty) = \kappa_0\delta_{ij}$.

For the purposes of later comparison we give also the renormalization group equation based on the above alternative slicing procedure for which

$$\delta D(q) = \delta t\ D(q)\,. \tag{36}$$

Because the addition of the extra slice takes us from $t \to t + \delta t$ we have after sorting out the overall sign

$$\frac{d\kappa_{ij}}{dt} = -\frac{\lambda_0^2}{\kappa_0^2}\int \frac{d^3q}{(2\pi)^3}D(q)\frac{\kappa_{im}q_m\ q_n\kappa_{nj}}{q_m\ \kappa_{mn}\ q_n}\,. \tag{37}$$

The prediction for the effective diffusivity tensor is $\kappa_{ij}(t = 1)$, obtained by integrating (37) with the boundary condition $\kappa_{ij}(t = 0) = \kappa_0\delta_{ij}$. In contrast to the situation in the isotropic case, the two predictions are not identical. We discuss the comparison between them and the results of a numerical simulation below.

In the above renormalization group calculation we have used the Ward identity instead of following the flow of the coupling tensor λ_{ij}, if instead one had explicitly carried out the tensorial vertex renormalization in the fashion of [4] one would have arrived at exactly the same renormalization group flow for κ_{ij} in the case where $\kappa_{0ij} \propto \lambda_{0ij}$. Hence the use of the Ward identity within the renormalization group calculation is entirely consistent.

8. Perturbative analysis of renormalization calculations

Equation (35) can be integrated perturbatively in powers of λ_0^2/κ_0^2. We set

$$\kappa_{ij} = \kappa_{ij}^{(0)} + \kappa_{ij}^{(1)} + \kappa_{ij}^{(2)} + \cdots \tag{38}$$

where

$$\kappa_{ij}^{(0)} = \kappa_0\delta_{ij}\,. \tag{39}$$

We find

$$\frac{d\kappa_{ij}^{(1)}}{d\Lambda} = \frac{\lambda_0^2}{\kappa_0^2} \int \frac{d^3 q}{(2\pi)^3} \delta(\Lambda - q) D(q) \frac{q_i\, q_j}{q^2} . \tag{40}$$

That is

$$\kappa^{(1)} = -\kappa_0 \frac{\lambda_0^2}{\kappa_0^2} \int \frac{d^3 q}{(2\pi)^3} \theta(q - \Lambda) D(q) \frac{q_i\, q_j}{q^2} . \tag{41}$$

On setting $\Lambda = 0$, we see that this result is identical with the perturbative one-loop result of (13). We now use this approximation to compute to the next order and obtain

$$\frac{d\kappa_{ij}^{(2)}}{d\Lambda} = \frac{\lambda_0^2}{\kappa_0^2} \int \frac{d^3 q}{(2\pi)^3} \delta(\Lambda - q) D(q) \left\{ \kappa_{im}^{(1)} \frac{q_m\, q_j}{q^2} + \frac{q_i\, q_n}{q^2} \kappa_{nj}^{(1)} - \frac{q_i\, q_j}{q^2} \frac{q_k \kappa_{kl}^{(1)} q_l}{q^2} \right\} . \tag{42}$$

On using (41) this equation can be integrated to give for the effective diffusivity

$$\kappa_{ij}^{(2)} = \kappa_0 \frac{\lambda_0^4}{\kappa_0^4} \int \frac{d^3 q}{(2\pi)^3} \frac{d^3 p}{(2\pi)^3} D(q) D(p) \theta(p - q) \times \left\{ \frac{p_i p_m}{p^2} \frac{q_m\, q_j}{q^2} + \frac{q_i\, q_n}{q^2} \frac{p_n p_j}{p^2} - \frac{q_i\, q_j}{q^2} \frac{q_k p_k p_l q_l}{q^2\, p^2} \right\} . \tag{43}$$

By dividing up these contributions and interchanging the dummy integration variables appropriately this result can be reorganized into the form

$$\kappa_{ij}^{(2)} = \kappa_0 \frac{\lambda_0^4}{\kappa_0^4} \left\{ \tfrac{1}{2} \rho_{im} \rho_{mj} + \chi_{ij} \right\} \tag{44}$$

where

$$\chi_{ij} = \frac{1}{2} \left\{ \int \frac{d^3 q}{(2\pi)^3} \frac{d^3 p}{(2\pi)^3} D(q) D(p) \theta(p - q) \frac{(p_i q_l - q_i p_l) q_l q_m p_m q_j}{q^4 p^2} + (i \leftrightarrow j) \right\} . \tag{45}$$

Note that

$$\chi_{ii} = 0 . \tag{46}$$

This result should be compared with that for ν_{ij} in (17). It is clear that although somewhat similar in structure $\chi_{ij} \neq \nu_{ij}$. The differences are the presence of the $\theta(p - q)$ factor and the replacement of the denominator factor $(p + q)^2$ by p^2.

The t-slicing method described above produces similar results except that the $\theta(p - q)$ factor is missing in the formula for χ_{ij}. Both renormalization group methods produce slightly different results at the two-loop level and both are different from the correct two-loop perturbation theory result. It must therefore be concluded that although the renormalization group method produces correct results to high order in the isotropic case, this is to a certain extent 'accidental'. It reflects the fact that the renormalization group method, based on any slicing procedure, only and inevitably computes iterations of one-loop contributions. The asymmetric case shows already in two-loop order that some multi-loop effects do not always factorize into single-loop ones.

9. Full renormalization group calculations

As opposed to the case where one has rotational invariance, the renormalization group equations for non-rotationally symmetric flows are much more difficult to integrate. The spatial structure of the correlation function becomes important and the corresponding equations require numerical integration. However, despite this, one simple result independent of the precise nature of the spatial correlation does remain. In both slicing techniques it is easy to show that

$$\mathrm{Tr}\log(\kappa_e) = -\frac{\lambda_0^2}{{\kappa_0}^2} + 3\log(\kappa_0)\,. \tag{47}$$

One may verify that, unlike the results for the individual components of the diffusion tensor, this result is entirely consistent with the results obtained from the two-loop perturbation theory. In the t-slicing method there is even a corresponding simple result for the running value of $\kappa(t)$,

$$\mathrm{Tr}\log(\kappa(t)) = -\frac{\lambda_0^2 t}{{\kappa_0}^2} + 3\log(\kappa_0)\,. \tag{48}$$

In this section we shall consider the two renormalization group techniques in the case where one has a matrix A of the form

$$A = \begin{pmatrix} \alpha & 0 & 0 \\ 0 & \alpha & 0 \\ 0 & 0 & \beta \end{pmatrix}. \tag{49}$$

Symmetry considerations imply that the form of the running diffusion tensor will therefore be given by

$$\kappa = \begin{pmatrix} \kappa & 0 & 0 \\ 0 & \kappa & 0 \\ 0 & 0 & \kappa' \end{pmatrix}. \tag{50}$$

The variables above being functions of t or Λ depending on the slicing method.

9.1. The t-slicing renormalization group

In what follows we shall set $\kappa_0 = 1$. The renormalization group equations can be reduced to the following:

$$\frac{\mathrm{d}\kappa}{\mathrm{d}t} = -\frac{\lambda_0^2\alpha\beta^{1/2}}{(2\pi)^{3/2}}\int \mathrm{d}^3q\,\exp\left[-\tfrac{1}{2}\alpha(q_1^2+q_2^2) - \tfrac{1}{2}\beta q_3^2\right]\frac{\kappa^2 q_1^2}{\kappa\left(q_1^2+q_2^2\right)+\kappa' q_3^2} \tag{51}$$

where

$$\kappa'(t) = \kappa^{-2}\exp(-\lambda_0^2 t)\,. \tag{52}$$

It is convenient to define the renormalization group flow in terms of the rescaled variables $\mu(t) = \kappa(t)/\alpha$ and $\mu'(t) = \kappa'(t)/\beta$. After some algebra the corresponding renormalization group equations can be shown to reduce to

$$\frac{\mathrm{d}\mu}{\mathrm{d}t} = -\lambda_0^2\mu' G\left[\left(1-\frac{\mu'}{\mu}\right)^{1/2}\right] \tag{53}$$

with

$$\mu'(t) = \frac{1}{\alpha^2\beta\mu^2(t)}\exp(-\lambda_0^2 t) \tag{54}$$

and the function G defined by

$$G(a) \equiv \frac{1}{2a^2(1-a^2)} + \frac{1}{4a^3}\log\left(\frac{1-a}{1+a}\right) \tag{55}$$

and its appropriate analytic continuation. The boundary condition is simply given by $\mu(0) = 1/\alpha$. The integration of this equation is now a relatively simple numerical task.

9.2. The momentum space renormalization group

By resorting to spherical polar coordinates within the integrands, the momentum slicing renormalization group, the renormalization group equations may be reduced to the following before resorting to numerical solution:

$$\frac{d\kappa}{d\Lambda} = \frac{\lambda_0^2}{(2\pi)^{1/2}}\alpha\beta^{1/2}\kappa^2\Lambda^2\exp\left(-\tfrac{1}{2}\alpha\Lambda^2\right)\int_0^1 du\ \exp\left(-\tfrac{1}{2}(\beta-\alpha)u^2\Lambda^2\right)\frac{1-u^2}{\kappa(1-u^2)+\kappa' u^2} \tag{56}$$

$$\frac{d\kappa}{d\Lambda} = \frac{2\lambda_0^2}{(2\pi)^{1/2}}\alpha\beta^{1/2}\kappa'^2\Lambda^2\exp\left(-\tfrac{1}{2}\alpha\Lambda^2\right)\int_0^1 du\,\exp\left(-\tfrac{1}{2}(\beta-\alpha)u^2\Lambda^2\right)\frac{u^2}{\kappa(1-u^2)+\kappa' u^2}. \tag{57}$$

For the purposes of numerical solution an upper cut-off for Λ is chosen so that the value of the right-hand sides of the above equations is zero within the numerical precision and the equations are integrated downward to $\Lambda = 0$.

10. Comparison with numerical simulation

The simulation procedure used in this paper is the same as that used in [4] which was based on the methods developed in [8, 7].

We shall begin the discussion of the efficacy of our various approximation schemes with a comparison of the measured value of $\mathrm{Tr}(\log(\kappa))$. The results of the numerical simulations for this quantity in the cases $A = \mathrm{diag}(1, 1, 4)$ and $A = \mathrm{diag}(1, 1, \frac{1}{4})$ are shown in figures 6 and 7, respectively, with the corresponding renormalization group predictions (which are the same for both methods and choices of A). The results show a very close agreement with the renormalization group predictions (comparable with the accuracy of the renormalization

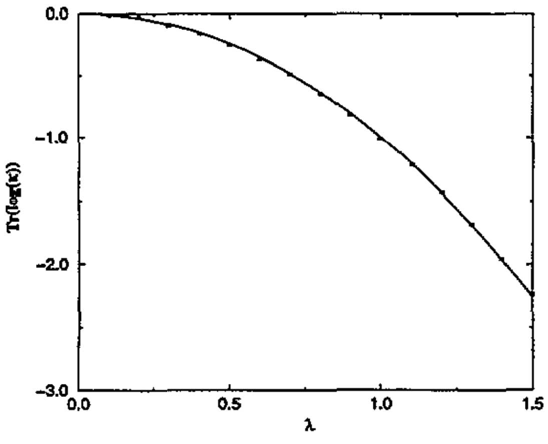

Figure 6. $\mathrm{Tr}(\log(\bar{\kappa}))$ versus renormalization group prediction for the case $A = \mathrm{diag}(1, 1, 4)$.

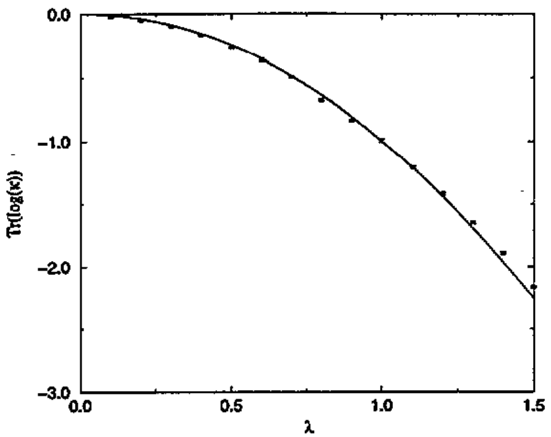

Figure 7. Tr (log(κ)) versus renormalization group prediction for the case $A = \mathrm{diag}(1, 1, 1/4)$.

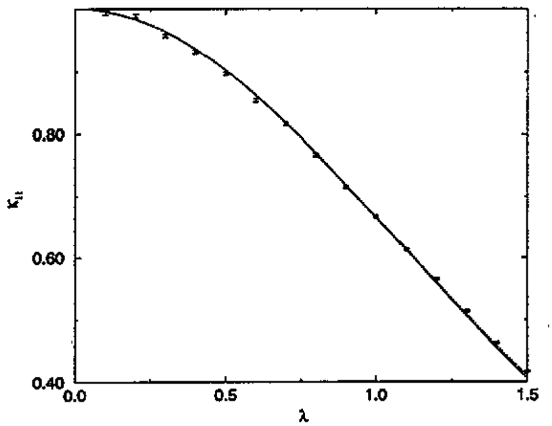

Figure 8. κ versus renormalization group predictions for the case $A = \mathrm{diag}(1, 1, 4)$, ($t$-slicing, full lines; momentum slicing, broken).

group calculations for the isotropic case examined in [4]. This agreement between the renormalization group predictions with the simulation and with two-loop perturbation theory leads one to speculate that (47) may be an exact result.

The results of the simulations for the individual components, κ_e and κ_e', are shown in figures 8–11. For large values of λ_0 we see that there is a departure between the both renormalization group techniques and the measured values. This is, of course, to be expected as we know that neither renormalization group technique agrees with the two-loop result. However, both techniques perform reasonably well, the momentum slicing method perhaps slightly better than the t-slicing one.

The inequalities in the values of κ_e and κ_e' can be simply understood from a physical point of view. The directions with the larger correlation length for the field ϕ can be regarded as smoother in that direction than those with the shorter correlation length and hence the diffusion constant is greater in these directions (i.e. the particle see a landscape which is relatively constant in directions with the greater correlation length but contains trapping maxima in the plane/line corresponding to the shorter correlation length). An extreme situation would be where $\beta \to \infty$ as α remains finite. In this case the correlation length in the z-direction has become infinite and hence even on very long time scales the field can be thought of as independent of z. The diffusion in the (x, y)-plane should become effectively two dimensional. Following this line of reasoning one should have that $\kappa_e' = 1$

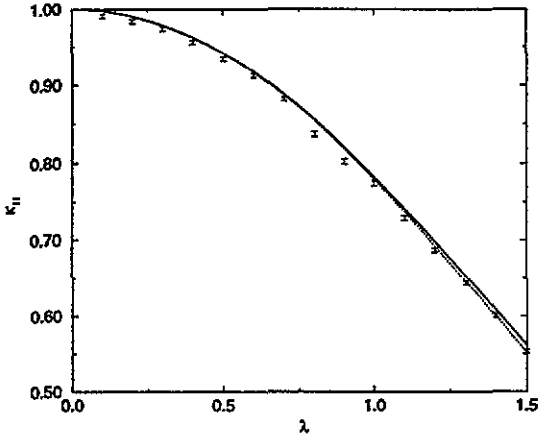

Figure 9. κ versus renormalization group predictions for the case $A = \mathrm{diag}(1, 1, 1/4)$, ($t$-slicing, full lines; momentum slicing, broken).

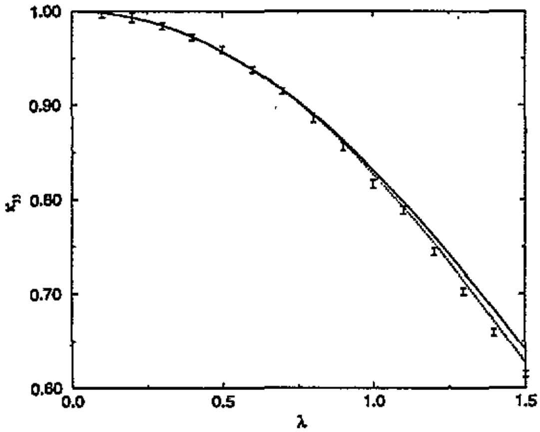

Figure 10. κ' versus renormalization group predictions for the case $A = \mathrm{diag}(1, 1, 4)$, ($t$-slicing, full lines; momentum slicing, broken).

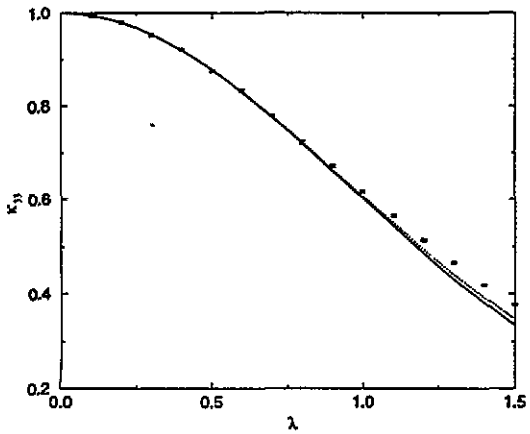

Figure 11. κ' versus renormalization group predictions for the case $A = \mathrm{diag}(1, 1, 1/4)$, ($t$-slicing, full lines; momentum slicing, broken).

and $\kappa_e = \exp(-\lambda_0^2/2)$ (if one believes the renormalization group calculation for the two-dimensional isotropic problem [4]). Putting this together implies the result $\mathrm{Tr}\log(\kappa) = -\lambda_0^2$, and hence there is an added consistency between (47) and the isotropic theory. Of course this argument is much more general and works in any number of dimensions, taking any subset of the correlation lengths to infinity whilst leaving the remaining correlation lengths all finite and equal.

One should also add that within the context of the above argument equation (19) is also entirely consistent. Clearly in the non-isotropic case (19) and (47) cannot be simultaneously true, in general. The fact that they are in agreement to $O(\lambda_0^4)$ means that only at quite high values of λ_0 could one see which is the more accurate. This is clearly a point that merits further investigation, but as was mentioned in [5] the simulation of these systems at high disorder presents technical difficulties in the measurements of the effective diffusion tensor.

11. Conclusions

In this paper we have examined methods for the evaluation of the effective diffusivity tensor for Brownian particles in a random gradient flow lacking rotational symmetry. In contrast with the isotropic version of the problem examined in [4–6], the resulting effective diffusion tensor depends explicitly on the nature of the spatial correlations of the Gaussian field (whereas before it just depended on the single-point variance). Moreover, in the case where the bare diffusion tensor and coupling constants are proportional to the identity, a perturbative analysis and a renormalization group analysis implies the proportionality of the effective diffusion tensor and the dressed coupling tensor, extending the Ward identity of [5] to a more general context.

The perturbation theory was developed to two-loops and then compared with two renormalization group methods. One method consisted of dividing the random field up as the sum/integral of infinitesimally small independent random fields and the other was based on the traditional momentum slicing method. In contrast with the isotropic case these two methods yield different results, nor do they agree with the two-loop perturbation theory result; hence they cannot be exact.

However, overall the agreement with numerical simulation is quite good. Furthermore both second order perturbation theory and both renormalization group methods are in agreement for the calculation of the object $\mathrm{Tr}\,(\log(\kappa))$ which is predicted to be $-\lambda_0^2/\kappa_0^2 + 3\log(\kappa_0)$. This is once again an object which is independent of the precise form of the correlation function for the random field ϕ and the agreement with the numerical simulations is very good.

Acknowledgments

This work was completed with the support from EU Grant CHRX-CT93-0411 and from Grant A93146 from the Leverhulme Trust.

References

[1] Bouchaud J-P and Georges A 1990 *Phys. Rep.* **195**
[2] Drummond I T and Horgan R R 1987 *J. Phys. A: Math Gen.* **20** 4661
[3] King P R 1994 *J. Phys. A: Math Gen.* **20** 3935
[4] Dean D S, Drummond I T and Horgan R R 1994 *J. Phys. A: Math Gen.* **27** 5135
[5] Dean D S, Drummond I T and Horgan R R 1995 *J. Phys. A: Math Gen.* **28** 1235
[6] Deem M W and Chandler D 1994 *J. Stat. Phys.* **76** 911
[7] Kraichnan R H 1976 *J. Fluid Mech.* **77** 753
[8] Drummond I T, Duane S and Horgan R R 1984 *J. Fluid Mech.* **138** 75
[9] Dean D S 1993 Stochastic dynamics *PhD Thesis* University of Cambridge